This is the accepted manuscript made available via CHORUS. The article has been published as:

Repulsive atomic Fermi gas with Rashba spin-orbit coupling: A quantum Monte Carlo study

Alberto Ambrosetti, Pier Luigi Silvestrelli, Francesco Pederiva, Lubos Mitas, and Flavio Toigo

Phys. Rev. A **91**, 053622 — Published 26 May 2015

DOI: 10.1103/PhysRevA.91.053622

Repulsive Atomic Fermi Gas with Rashba Spin-Orbit Coupling: a Quantum Monte Carlo Study

Alberto Ambrosetti[1],* Pier Luigi Silvestrelli[1], Francesco Pederiva[2], Lubos Mitas[3], and Flavio Toigo[1]
1) Dipartimento di Fisica, University of Padova, via Marzolo 8, I–35131, Padova, Italy.
2) Dipartimento di Fisica e LISC, Università di Trento, Via Sommarive 14, I–38123, Povo, Trento, and Trento Institute for Fundamental Physics and Applications, Trento, Italy
3) Department of Physics, North Carolina State University, Raleigh, North Carolina 27695-8202, USA

Thanks to the recent experimental realization and control of artificial gauge fields, Spin-orbit (SO) couplings are witnessing an ever increasing interest in the field of cold atoms. However, predicting their effect on spin polarization and energetic properties of interacting systems is a major challenge, due to the complex interplay between spin and position dynamics. In this work we exploit the Diffusion Monte Carlo algorithm to compute energetic and polarization properties of a three dimensional repulsive Fermi gas in the presence of Rashba spin-orbit coupling. We find that SO effects tend to contrast the spin alignment induced by the exchange interaction, slightly shifting the onset of the Stoner instability towards larger values of the scattering length. In addition, polarization and energy properties of the system can be tuned trough a combined control of the repulsive interaction and Rashba coupling.

PACS numbers:

The Fermi gas with contact or finite-range repulsion is a prototypical model system. Due to its nontrivial magnetic properties, it has been a subject of numerous investigations over the years[1–7]. The corresponding Hamiltonian (Stoner model), introduced in order to describe itinerant ferromagnetism in an electron gas with screened two-body Coulomb interaction [8], was shown to yield a spin polarization transition upon control of the two-body repulsion strength[3–5]. In addition, the peculiar magnetic behavior of the model was also confirmed for trapped configurations, where the problem of stability and phase separation of a two-component Fermi gas was theoretically addressed[1, 9, 10].

According to mean field theoretical predictions[4], a polarization transition can be triggered in the system by enhancing the repulsive interaction above a critical value. The critical scattering length is determined by a competition between the kinetic energy and the interaction among fermions having opposite spin. Notably, both the inclusion of higher order perturbative terms and Quantum Monte Carlo lead to results in qualitative agreement with the mean field picture, although predicting a different value of the critical interaction[3, 5, 6].

While the physics of the Stoner model appears to be qualitatively well understood, the effect of adding the Spin-Orbit (SO) coupling is less certain. In particular, it might lead to sizable modifications of the polarization properties of the system. One specific form of the spin-orbit coupling is the Rashba SO interaction[11–14]

$$V_{SO} = \lambda \left(p_y \sigma_x - p_x \sigma_y \right), \tag{1}$$

where σ_i is the i-th Pauli matrix and p_i is the i-th component of the momentum operator. This interaction has been widely studied in the field of low-dimensional semiconductor systems. Recently, it has also been realized in ultracold atomic systems in combination with a Dresselhaus[15] coupling by means of controlled laser beams[16–19], and it is currently witnessing increasing attention. In fact, due to its tunable strength[20] through the parameter λ, the Rashba SO coupling may allow for an otherwise challenging fine tuning of the system polarization.

Motivated by the remarkable experimental achievements, a significant amount of recent theoretical work has been focused on the effects of Rashba or Dresselhaus SO couplings in Bose-Einstein condensates[21–29], and in superfluid fermions at the BCS-BEC crossover[30–49]. A very recent mean field variational study of the two dimensional Fermi gas with Rashba coupling[50] has indeed shown how SO effects can macroscopically influence the Stoner instability, leading to partially magnetized states. However, while a detailed theoretical understanding of the repulsive Fermi gas in presence of Rashba interaction would be extremely appealing, the intrinsically challenging calculations beyond the mean field are further complicated by the non-local nature of the SO coupling[50].

In the present paper we address this problem using an accurate Diffusion Monte Carlo (DMC) algorithm to predict the energetic and polarization properties of the three dimensional (3D) Fermi gas. In order to correctly treat SO interactions, a suitable imaginary time spin-orbit propagator is introduced, following our previous work in the context of the two-dimensional electron gas and circular quantum dots[51, 52].

In particular, DMC has enabled us to calculate accurate estimates of ground state properties of the Hamiltonian with a soft-sphere (SS) repulsion and Rashba spin-orbit interaction. We find that the Rashba interaction tends to frustrate the system polarization, reducing its value, and shifting its onset to slightly higher values

*Electronic address: alberto.ambrosetti@unipd.it

of the repulsive interaction scattering length a. While macroscopic polarization is found only above a critical scattering length a_c, the present results cannot exclude the onset of a weaker polarization below a_c, opening thus new questions about the order of the transition.

The paper is organized as follows: in section I the method is presented along with the details of the imaginary time spin-orbit propagator. In section II the trial wave function of choice is introduced together with motivation for its spinorial structure. Finally, in section III, the QMC results for polarization and energetic properties are reported and discussed.

I. METHODS

A. Quantum Monte Carlo for SO Hamiltonians

Diffusion Monte Carlo (DMC) is a highly accurate technique, based on projecting out the ground state component of an initial arbitrary state of the system (not orthogonal to the ground state itself) by means of the iterated application of an imaginary time (τ) propagation. The quantum state is approximated by a finite expansion on position eigenstates, i.e. by a collection of points in configuration space:

$$|\Psi\rangle \sim \sum_k |X_k\rangle\langle X_k|\Psi\rangle. \tag{2}$$

Notice that in this case the configurations have to be intended in an extended meaning, therefore including all the relevant degrees of freedom (e.g. position and spin). Each of these points is evolved according to a short-time approximation of the imaginary time propagator associated with the Hamiltonian H:

$$\langle X_k|\Psi\rangle = \sum_l \langle X_k|e^{-\Delta\tau(H-E_0)}|X'_l\rangle\langle X'_l|\Psi\rangle,$$

where E_0 is a constant introduced to preserve the normalization of the ground state, and k is the configuration index. In the limit of an infinite iteration, this propagation leads to ground-state projection (power method).

Following our previous work[51, 52], the Hamiltonian is split into three terms, namely kinetic energy T, repulsive two-body interaction V_{SS} and SO contribution V_{SO}.

$$H = T + V_{SS} + V_{SO}\,. \tag{3}$$

Making use of the Trotter's formula, the imaginary time Green's function is then approximated (at order $O(\Delta\tau)$) as

$$e^{-\Delta\tau H} \simeq e^{-\Delta\tau V_{SS}}\, e^{-\Delta\tau V_{SO}}\, e^{-\Delta\tau T}. \tag{4}$$

The rightmost factor corresponds to the imaginary time free particle Gaussian propagator

$$G_0\left(\mathbf{R}', \mathbf{R}, \Delta\tau\right) = (2\pi\Delta\tau)^{-N} \exp\left[-\frac{(\mathbf{R}'-\mathbf{R})^2}{2\Delta\tau}\right], \tag{5}$$

from which space coordinates displacements $\mathbf{R}'-\mathbf{R}$ are sampled ($\mathbf{R}$ indicates here the collective space coordinates of the system). The second factor (containing V_{SO}) is subsequently applied to G_0. The momentum operators at the exponent act as derivatives with respect to the coordinates $\mathbf{R}', \mathbf{R}$, and after some algebra the SO and kinetic parts of the imaginary time propagator read:

$$\begin{aligned} e^{-V_{SO}}\, G_0\left(\mathbf{R}', \mathbf{R}, \Delta\tau\right) &\simeq \\ &= e^{-i\lambda\sum_{i=1}^{N}(\Delta r_i^y \sigma_i^x - \Delta r_i^x \sigma_i^y)} G_0\left(\mathbf{R}', \mathbf{R}, \Delta\tau\right), \end{aligned} \tag{6}$$

where Δr_i^a $(a = x, y)$ indicates the space displacement along the x, y direction of the i-th particle. The remaining part of the propagator, depending on the local V_{SS} interaction, finally contributes as a conventional local "weighting" factor. Hence, by taking into account the necessary normalization factors, the whole imaginary time Green's function reads:

$$\begin{aligned} G\left(\mathbf{R}', \mathbf{R}, \Delta\tau\right) &= e^{-[V_{SS}(\mathbf{R}) - E_0 - N\lambda^2]\Delta\tau} \\ &\times e^{-i\lambda\sum_{i=1}^{N}(\Delta r_i^y \sigma_i^x - \Delta r_i^x \sigma_i^y)} G_0\left(\mathbf{R}', \mathbf{R}, \Delta\tau\right). \end{aligned} \tag{7}$$

Since the SO propagator acts on the particle spin through the Pauli matrices σ_x and σ_y, the spin variables are modified along the simulation, and must be considered as dynamic variables. As in standard Diffusion Monte Carlo, we make use of a variational ansatz to serve as an importance function guiding the sampling process. Due to the presence of spin rotations, this "trial" wave function Ψ_T will generally be complex. This adds a further complication with respect to the standard QMC treatment of many fermion systems. In particular, it is not possible to use the standard fixed-node algorithm to circumvent the so-called sign problem, and enforce the antisymmetry of the ground state. We need instead to use a fixed-phase constraint[53–55]. In order to minimize finite size errors and achieve a smoother variability of the energy with respect to polarization, twist-averaged boundary conditions were implemented, according to the prescriptions of Ceperley and coworkers[56]. Using these developments, the DMC method then typically provides very accurate energies and expectation values of operators which commute with the Hamiltonian. In the present case, however, given the non commutativity of σ_z with V_{SO}, a particular attention should be given to the evaluation of the system polarization. In fact, since the DMC method samples the mixed distribution $\Psi_T\Psi_{DMC}$ (not Ψ^2_{DMC}), in the case of a non-commuting quantity O, a straightforward DMC estimate would lead to the so-called mixed estimator $\langle O\rangle_{mix} = \langle\Psi_T|O|\Psi_{DMC}\rangle$. It is thus common to correct the mixed estimator by partial elimination of the bias at the second order of the difference between the trial and exact eigenstates as given by the equation[57]

$$\langle O\rangle_{corr-mix} = 2\langle O\rangle_{mix} - \langle O\rangle_{VMC} + \mathcal{O}(\Psi_T - \Psi_{exact})^2\,. \tag{8}$$

The first term on the right hand side of the equation above represents the DMC mixed estimate of the expectation value of the operator O, while the second term is

the variational Monte Carlo (VMC) estimate. This difference therefore reduces the bias from the importance function to the second order in the difference between the importance and the ground state wave functions. For this reason, Eq.(8) will be addressed in the following as *corrected mixed* estimator.

As already mentioned, in presence of SO interaction the fermion spin cannot be fixed and must be explicitly treated as a variable in the stochastic dynamics, both for VMC and DMC calculations. In particular, we will apply here a recently developed algorithm[58], which is based on the integration of continuous auxiliary variables.

B. Fermion-Fermion interaction

As concerns the detailed realization of two-body finite-range interaction potential, this is modeled in the present work as a soft sphere potential acting between couples of Fermions having opposite spins:

$$V_{SS} = \sum_{i>j} v_{ss}(|\mathbf{r_i} - \mathbf{r_j}|)\frac{1 - \bar{\sigma}_i \cdot \bar{\sigma}_j}{2}\,. \tag{9}$$

Here $\bar{\sigma}_i$, indicates the spin matrices relative to the i-th particle, and can be expressed as $(\sigma_x, \sigma_y, \sigma_z)_i$, while $v_{ss}(r)$ is defined as

$$v_{ss}(r) = V_0\Theta(R_0 - r)\,, \tag{10}$$

where r is positive by definition. The Heaviside step function $\Theta(R_0 - r)$ limits the range of the potential to R_0, while the potential height V_0 is set in a way to recover the correct value of a, according to the relation

$$a = R_0\big[1 - \frac{\mathrm{tgh}\kappa R_0}{\kappa R_0}\big]\,, \tag{11}$$

where $\kappa^2 = mV_0$. Experimentally, the scattering length can be accurately controlled, for instance by exploiting the Feshbach resonance mechanism[59, 60].

II. WAVE FUNCTION

Since the present work is concerned with the simulation of interacting fermions, the quality of of the trial wave function Ψ_T becomes especially important. In fact, the phase that will be enforced by the fixed phase DMC algorithm will depend on the choice of Ψ_T, influencing thus the accuracy of the final results. In this regard, previous work on the two-dimensional electron gas[52] pointed out the need to explicitly account for the non trivial spin-dependence induced by V_{SO} in the independent particle states. This problem was solved by making use of single particle spinors which diagonalize the Hamiltonian of the non-interacting fermions $T + V_{SO}$:

$$\phi(\mathbf{r})_{\mathbf{k}\pm} = e^{i\mathbf{k}\cdot\mathbf{r}}\chi_{\mathbf{k}\pm}\,. \tag{12}$$

where

$$\chi_{\mathbf{k}\pm}(\mathbf{r}) = \frac{1}{\sqrt{2}}\begin{pmatrix}\pm\frac{k_y + ik_x}{k}\\ 1\end{pmatrix}. \tag{13}$$

The above spinors already account for a good amount of the non-locality induced by the SO coupling. However, the expectation of σ_z on any of these single-particle states is identically zero. In order to retain information on the non-local spin structure and simultaneously allow for non-zero polarization, we make use of the following spinorial form [50]

$$\chi_{\mathbf{k}\pm,h}(\mathbf{r}) = c_{\pm,h}(\mathbf{k})\frac{1}{\sqrt{2}}\begin{pmatrix}\frac{\lambda(k_y + ik_x)}{h\pm\sqrt{h^2+\lambda^2k^2}}\\ 1\end{pmatrix}, \tag{14}$$

where $c_{\pm,h}(\mathbf{k})$ is a normalization factor defined through the condition

$$c^2_{\pm,h}(\mathbf{k})\left(\frac{\lambda^2k^2}{(h^2 \pm \sqrt{h^2+\lambda^2k^2})^2} + 1\right) = 1\,. \tag{15}$$

This functional form, depending on the Rashba SO strength λ and on a second parameter h, can be inferred from the eigenvectors of a single-particle Hamiltonian including V_{SO} and an external potential of the form $h\sigma_z$. However, in the physical case considered, the external field is an electric-like field, parameterized by the SO coupling strength λ. The quantity h instead is simply a variational parameter which modifies the spinorial structure of the wave function, *interpolating* between the Rashba eigenstates ($h = 0$) and the eigenstates of σ_z ($h \to \infty$).

Making use of the above single particle orbitals, a single Slater determinant is constructed. No explicit two-body correlation (e.g in form of a Jastrow factor) is thus included in the trial wave function. This choice might imply a somewhat slower convergence of the energy with respect to the number of steps, but it does not interfere with the quality of the phase structure of the function, which is the only feature affecting the accuracy of the projected energy.

III. RESULTS

A. QMC Results

The present quantum Monte Carlo simulations were performed with a reference population of 300 walkers and a time step of 0.002 (units are indicated below), making use of 66 particles confined in a periodically repeated cubic box. Convergence with respect to the time step and the number of walkers was achieved within the statistical error. The non-interacting Fermi momentum k_F used throughout the manuscript is defined as $k_F = (3\pi^2 n)^{1/3}$, where n is the total density of the system. Energies are expressed in units of E_P, namely the energy of the fully spin-polarized system, defined as $(6\pi^2 n)^{5/3}/(20\pi^2 m)$. The repulsive potential range R_0

was set to 2.8 the scattering length, and V_0 was accordingly computed. The Rashba coupling λ is given in units of $\frac{\hbar}{ml}$, where m is the atomic mass and l is a length scale defined as $(\frac{3}{4\pi n})^{1/3}$. Three different values of λ were considered, namely $\lambda = 0$ (absence of SO interaction), $\lambda = 0.15$ and $\lambda = 0.30$. The total DMC energy was minimized with respect to the single-particle states occupation, and with respect to the parameter h, optimizing the trial wave function at every given value of the scattering length and of the SO coupling.

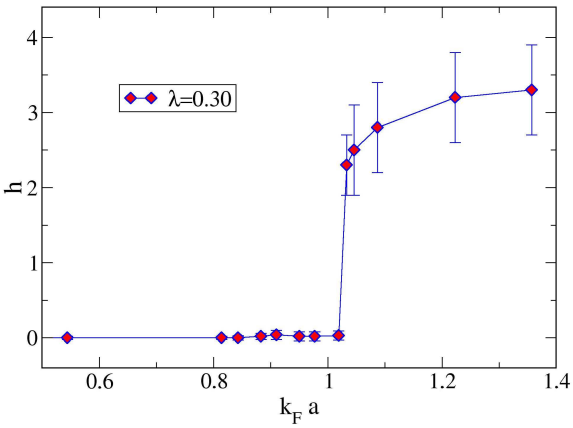

FIG. 1: Optimal h as a function of the scattering length at $\lambda = 0.3$.

Calculations confirm the importance of a variational optimization of the spinorial structure of the trial wave function. Fig. 1 shows the optimal h value at finite λ. It varies as a function of the scattering length, increasing with the strength of the 2-body repulsion, with a sudden jump that corresponds to the polarization transition. This behavior is consistent with the mean field picture of Ref.[50], where non-zero polarization is developed in correspondence of a sudden increase of the variational parameter h. In fact, a finite value of h indicates a tendency of the system to choose a preferred spin orientation, inducing a non-zero polarization in the system.

The z spin polarization P is calculated using the *corrected mixed* estimate of the operator

$$P = \frac{1}{N}\sum_{i}^{N} \sigma_z^i. \qquad (16)$$

The computed values confirm the presence of spin polarization at large values of the scattering length.

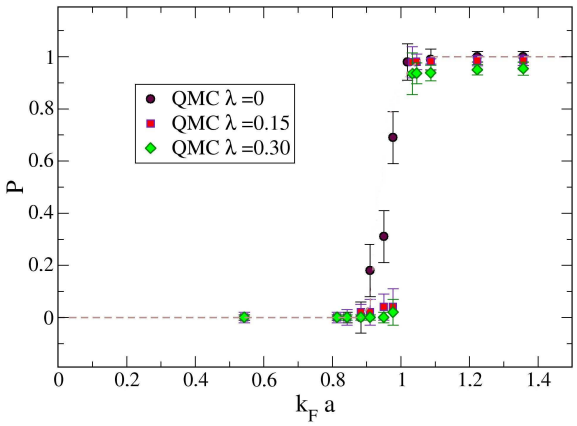

FIG. 2: Polarization of Fermi gas along the z direction as a function of the two-body interaction scattering length a. Results are given in absence of SO interaction ($\lambda = 0$) and for two different Rashba interaction strengths ($\lambda = 0.15, 0.30$).

Fig.2 shows that in absence of SO interaction the critical point is located near $k_F a_c \sim 0.85$, in good agreement with previous QMC predictions for soft sphere contact interaction[5], and with a second order approximate estimate[3].

While a mean field description predicts a discontinuity of the P derivative with respect to $k_F a$,[5] we observe that correlation effects slightly modify the relation between P and $k_F a$, making the transition less steep at criticality. Due to the statistical error, however, it is not yet possible to establish whether correlation terms modify the nature of the Stoner instability, possibly turning it into a higher order transition.

Notably, when considering finite Rashba couplings, the onset of the polarization transition is shifted to larger $k_F a$. Moreover, while at $\lambda = 0$ the present results are compatible with complete polarization at $k_F a \sim 1.1$, $P < 1$ is found also in this regime for finite SO couplings. Hence, the overall effect of the Rashba interaction is that of reducing the spin polarization of the system. This fact can be understood in terms of the spin precession induced by the SO coupling. Since the Rashba coupling lowers the single particle energies, a competition with the two-body interaction energy will take place: in fact the spin alignment unavoidably alters the non-local spin texture, contrasting the overall effect of the SO coupling. Observing Fig.2, however, the polarization at finite λ tends to be closer and closer to 1 at large scattering lengths. In fact, for $k_F a \to \infty$ full polarization is expected, given the overwhelming effects of the two-body repulsion. Remarkably, qualitatively analogous results were found also in the two-dimensional gas[50], making use of a variational procedure based on single particle spinors of the form of Eq. (14). We also emphasize that the polarization reduction found above criticality at finite λ might

open the way to a fine tuning of the degree of polarization by means of an externally controlled SOC, therefore despite its apparent complexity this task can be actually achieved through a simple control of the scattering length at the critical point.

In order to better understand the polarization transition and its relation to the spinorial structure of the single particle wave functions, in Fig.3 we plot the DMC energy as a function of the variational parameter h at different values of the two-body interaction and fixed λ. At low scattering lengths a single minimum at $h = 0$ is present, while for increasing the two-body repulsion a local minimum appears at higher h. Beyond criticality, the second minimum becomes the global minimum, until the minimum at $h = 0$ disappears. Interestingly, at large values of h, the system tends to fully polarize, and the energy is expected to gradually approach the non-interacting limit E_P.

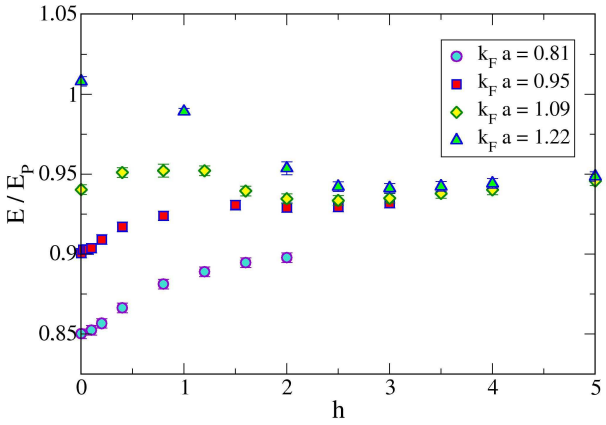

FIG. 3: DMC energies as a function of h at different values of the two body interaction strength. The Rashba interaction coupling is fixed here to $\lambda = 0.3$.

In Fig.4 we report the ground state energy as a function of the scattering length for the selected λ values. As in the single-particle picture, the SO coupling causes a net decrease of the energy, which becomes more evident at larger λ. While in absence of SO coupling the DMC results rapidly approach the fully polarized non-interacting limit E_P, at finite λ a residual SO energy effect persists. As visible from Fig.4, however, the energy difference between the data sets in presence and in absence of Rashba coupling clearly diminishes at large scattering lengths, a behavior which is consistent with the aforementioned tendency of the system to develop full polarization at $k_F a \to \infty$. In fact, also in this case, one expects that at large a the energy will approach E_P: at full polarization the non local Rashba spin texture is lost, and a single particle picture clearly suggests that the expectation value of V_{SO} vanishes if all spins are aligned along z.

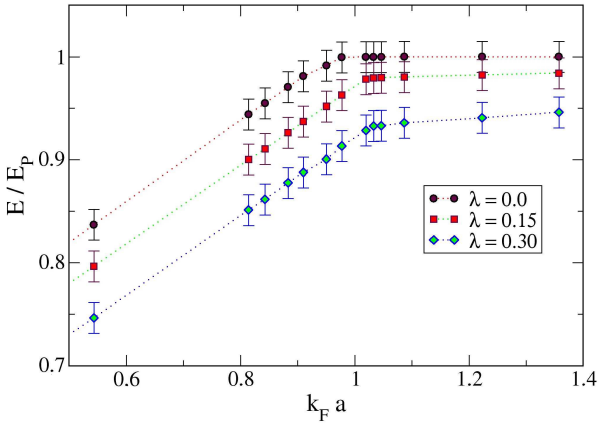

FIG. 4: DMC energies (in units of E_P) as a function of the scattering length at different Rashba coupling strengths ($\lambda = 0, 0.15, 0.30$).

For the sake of completeness we remark that the adopted trial wave function is well suited for the description of z-polarization. A detailed investigation of the possible $x - y$ polarization effects, instead, would require a different form of the single-particle spinors. Clearly, in-plane polarization components would deserve a detailed analysis, which is beyond the scope of the present article. As a comment, however, the development of polarization in the $x - y$ plane would require a substantial modification of the Fermi surface. In particular, according to a mean-field description, a non symmetric and anisotropic occupation of single particle states turns out to be necessary. Due to the related kinetic energy increase, such polarization effects are not expected to be favored with respect to the z component considered here. We also point out that different SO couplings may have different effects on the polarization properties of the system. In the case of equal Rashba and Dresselhaus couplings, for instance, the single-particle spinorial structure is independent on momentum. Hence, no major difference with respect to the standard Stoner model is expected, at variance with the pure Rashba coupling considered here.

IV. CONCLUSIONS

We performed QMC calculations of the spin and energetic properties of the 3D repulsive Fermi gas in the presence of Rashba SO coupling. Interestingly, correlation effects seem to induce a smoother polarization transition at the critical point. The inclusion of Rashba SO coupling causes an overall depolarization of the system, and shifts the critical point to slightly higher values of the scattering length. At the same time, partially polarized

states are developed well beyond criticality in presence of Rashba coupling, opening the way to a fine tuning of the system polarization. The energy is also visibly reduced by the SO coupling, however, the asymptotic behavior of the QMC data suggest that at infinite scattering lengths the two-body repulsion should prevail over the non-local structure induced by the SO coupling, recovering the fully polarized non-interacting limit.

V. ACKNOWLEDGEMENTS

A.A. acknowledges Luca Salasnich for useful discussions and fruitful suggestions. Work of L.M. was supported by the U.S. Department of Energy (DOE), Office of Science, Basic Energy Sciences (BES) under Award DE-SC00012314.

[1] G. J. Conduit, Phys. Rev. A **82** 043604 (2010).
[2] G. J. Conduit and B. D. Simons, Phys. Rev. A **79** 053606 (2009).
[3] G. J. Conduit, A. G. Green and B. D. Simons, Phys. Rev. Lett. **103** 207201 (2009).
[4] R. A. Duine and A. H. MacDonald, Phys. Rev. Lett **95**, 230403 (2005).
[5] S. Pilati , G. Bertaina, S. Giorgini, M. Troyer, Phys. Rev. Lett. **105** , 030405 (2010).
[6] S.-Y. Chang, M. Randeria, and N. Trivedi, Proc. Natl. Acad. Sci. bf 108 51 (2010).
[7] E. Fratini and S. Pilati, Phys. Rev. A **90**, 023605 (2014).
[8] E.C. Stoner, Rep. Prog. Phys. **11**, 43 (1947).
[9] L. Salasnich, B. Pozzi, A. Parola, and L. Reatto, J. Phys. B 33, 3943 (2000)
[10] T. Sogo and H. Yabu, Phys. Rev. A 66, 043611 (2002)
[11] Y.A. Bychkov and E.I. Rashba, J. Phys. C **17**, 6029 (1984).
[12] L. P. Kouwenhoven, T. H. Oosterkamp, M. W. S. Danoesastro, M. Eto, D. G. Austing, T. Honda, S. Tarucha, Science,**278** 1788 (1997).
[13] D. R. Steward, D. Sprinzak, C. M. Marcus, C. I. Duruöz, J. S. Harris Jr., Science, **278** 1784 (1997).
[14] G. Engels, J. Lange, T. Schäpers and H. Lüth , Phys. Rev. B **55**, R1958 (1997).
[15] G. Dresselhaus, Phys. Rev. **100**, 580 (1955).
[16] G. Juzeliunas, J. Ruseckas, J. Dalibard, Phys. Rev. A **81**, 053403 (2010); J. Dalibard, F. Jerbier, G. Juzeliunas, P. Öhberg, Arxiv-Cond.Matt. 1008.5378 (2010).
[17] Y.-J. Lin, K. Jimenez-Garcia, and I. B. Spielman Nature Lett. **471**, 83 (2011).
[18] J.-Y. Zhang, S.-C. Ji, Z. Chen, L. Zhang, Z.-D. Du, B. Yan, G.-S. Pan, B. Zhao, Y.-J. Deng, H. Zhai, S. Chen, and J.-W. Pan., Phys. Rev. Lett.**109**, 115301 (2012).
[19] P. Wang, Z.-Q. Yu, Z. Fu, J. Miao, L. Huang, S. Chai, H. Zhai, and J. Zhang, Phys. Rev. Lett. **109**, 095301 (2012).
[20] M. Kohda, T. Nihei, J. Nitta,*Physica E* **40** 1194 (2008).
[21] Y. Li, L.P. Pitaevskii, and S. Stringari, Phys. Rev. Lett.**108**, 225301 (2012).
[22] G.I. Martone, Yun Li, L.P. Pitaevskii, and S. Stringari,Phys. Rev. A i**86**, 063621 (2012).
[23] M. Burrello and A. Trombettoni, Phys. Rev. A **84**,043625 (2011).
[24] M. Merkl, A. Jacob, F. E. Zimmer, P. Ohberg, and L. Santos, Phys. Rev. Lett. **104**, 073603 (2010).
[25] O. Fialko, J. Brand, and U. Zulicke, Phys. Rev. A **85**, 051605 (2012); R. Liao, Z.-G. Huang, X.-M. Lin, and W.-M. Liu, ibid. **87**, 043605 (2013).
[26] Y. Xu, Y. Zhang, and B. Wu, Phys. Rev. A **87**, 013614 (2013).
[27] L. Salasnich and B.A. Malomed, Phys. Rev. A **87**, 063625 (2013).
[28] X.-Q. Xu and J. H. Han, Phys. Rev. Lett. **107**, 200401 (2011); S. Sinha, R. Nath, and L. Santos, Phys. Rev. Lett. **107**, 270401(2011); C.-F. Liu and W. M. Liu, Phys. Rev. A **86**, 033602 (2012); E. Ruokokoski, J. A. M. Huhtamaki, and M. Mottonen, Phys. Rev. A **86**, 051607 (2012); H. Sakaguchi, and B. Li, Phys. Rev. A **87**, 015602 (2013).
[29] Y. Deng, J. Cheng, H. Jing, C. P. Sun, and S. Yi, Phys. Rev. Lett. **108**, 125301 (2012).
[30] J. P. Vyasanakere and V. B. Shenoy, Phys. Rev. B **83**, 094515 (2011).
[31] J. P. Vyasanakere, S. Zhang, and V. B. Shenoy, Phys. Rev. B **84**, 014512 (2011).
[32] M. Gong, S. Tewari, and C. Zhang, Phys. Rev. Lett. **107**, 195303 (2011).
[33] H. Hu, L. Jiang, X-J. Liu, and H. Pu, Phys. Rev. Lett. **107**, 195304 (2011).
[34] Z-Q. Yu and H. Zhai, Phys. Rev. Lett. **107**, 195305 (2011).
[35] M. Iskin and A. L. Subasi, Phys. Rev. Lett. **107**, 050402 (2011).
[36] W. Yi and G.-C. Guo, Phys. Rev. A **84**, 031608 (2011).
[37] L. DellAnna, G. Mazzarella, and L. Salasnich, Phys. Rev. A **84**, 033633 (2011).
[38] M. Iskin and A. L. Subasi, Phys. Rev. A **84**, 043621 (2011).
[39] J. Zhou, W. Zhang, and W. Yi, Phys. Rev. A, **84**, 063603 (2011).
[40] L. Jiang, X.-J. Liu, H. Hu, and H. Pu, Phys. Rev. A **84**, 063618 (2011).
[41] Li Han and C.A.R. Sa de Melo, Phys. Rev. A **85**, 011606(R) (2012).
[42] G. Chen, M. Gong, and C. Zhang, Phys. Rev. A **85**, 013601 (2012).
[43] K. Zhou, Z. Zhang, Phys. Rev. Lett. **108**, 025301 (2012).
[44] X. Yang, S. Wan, Phys. Rev. A **85**, 023633 (2012).
[45] M. Iskin, Phys. Rev. A **85**, 013622 (2012).
[46] K. Seo, L. Han, C.A.R. Sa de Melo, Phys. Rev. A **85**, 033601 (2012).
[47] L. He and Xu-Guang Huang, Phys. Rev. Lett. **108**, 145302 (2012).
[48] X.J. Liu, M.F. Borunda, X. Liu, J. Sinova, Phys. Rev. Lett. **102**, 046402 (2009).
[49] L.W. Cheuk et al., Phys. Rev. Lett. **109**, 095302 (2012).
[50] A. Ambrosetti, G. Lombardi, L. Salasnich, P.L. Silvestrelli, F. Toigo, Phys. Rev. A **90** 043614 (2014).
[51] A. Ambrosetti, F. Pederiva, and E. Lipparini *Phys. Rev. B* **83** 155301 (2011).
[52] A. Ambrosetti, F. Pederiva, E. Lipparini, and S. Gandolfi *Phys. Rev. B* **80** 125306 (2009).

[53] S. Gandolfi, A. Y. Illarionov, K. E. Schmidt, F. Pederiva, and S. Fantoni, Phys. Rev. C **79** 054005 (2009).
[54] F. Bolton, Phys. Rev. B **54** 4780 (1996).
[55] L. Colletti, F. Pederiva, E. Lipparini, and C. J. Umrigar, Eur. Phys. J. B **27** 385 (2002).
[56] C. Lin, F. H. Zong, and D. M. Ceperley, Phys. Rev. E **64** 016702 (2001).
[57] A. Badinski,P. D. Haynes, and R. J. Needs,Phys. Rev. B **77** 085111 (2008).
[58] A. Ambrosetti, P. L. Silvestrelli, F. Toigo, L. Mitas, and F. Pederiva, Phys. Rev. B **85** 045115 (2012).
[59] H. Feshbach, Ann. Phys. **5** 357 (1958).
[60] C. Chin, R. Grimm, P. Julienne, and . Tiesinga, Rev. Mod. Phys. **82** 1225 (2010).